

# Double chromodomains cooperate to recognize the methylated histone H3 tail

John F. Flanagan<sup>1</sup>, Li-Zhi Mi<sup>2†</sup>, Maksymilian Chruszcz<sup>3</sup>, Marcin Cymborowski<sup>3</sup>, Katrina L. Clines<sup>1</sup>, Youngchang Kim<sup>4</sup>, Wladek Minor<sup>3</sup>, Fraydoon Rastinejad<sup>1,2</sup> & Sepideh Khorasanizadeh<sup>1</sup>

Chromodomains are modules implicated in the recognition of lysine-methylated histone tails and nucleic acids<sup>1,2</sup>. CHD (for chromo-ATPase/helicase-DNA-binding) proteins regulate ATP-dependent nucleosome assembly and mobilization through their conserved double chromodomains and SWI2/SNF2 helicase/ATPase domain<sup>3–5</sup>. The *Drosophila* CHD1 localizes to the interbands and puffs of the polytene chromosomes, which are classic sites of transcriptional activity<sup>6</sup>. Other CHD isoforms (CHD3/4 or Mi-2) are important for nucleosome remodelling in histone deacetylase complexes<sup>7,8</sup>. Deletion of chromodomains impairs nucleosome binding and remodelling by CHD proteins<sup>4</sup>. Here we describe the structure of the tandem arrangement of the human CHD1 chromodomains, and its interactions with histone tails. Unlike HP1 and Polycomb proteins that use single chromodomains to bind to their respective methylated histone H3 tails, the two chromodomains of CHD1 cooperate to interact with one methylated H3 tail. We show that the human CHD1 double chromodomains target the lysine 4-methylated histone H3 tail (H3K4me), a hallmark of active chromatin<sup>9</sup>. Methylammonium recognition involves two aromatic residues, not the three-residue aromatic cage used by chromodomains of HP1 and Polycomb proteins<sup>10–13</sup>. Furthermore, unique inserts within chromodomain 1 of CHD1 block the expected site of H3 tail binding seen in HP1 and Polycomb, instead directing H3 binding to a groove at the inter-chromodomain junction.

We previously showed that the highly homologous chromodomains of HP1 and Polycomb proteins are discriminatory for binding to the methylated lysine 9 and lysine 27 in histone H3 (H3K9me and H3K27me), which are modifications associated with constitutive and facultative heterochromatin, respectively<sup>12</sup>. Unlike HP1 and Polycomb, the CHD1 protein contains tandem chromodomains and is present in sites of transcriptional activity in *Drosophila*<sup>6</sup>. In yeast, CHD1 was identified in the SAGA/SLIK histone acetyltransferase complexes, and chromodomain 2 has been suggested to be responsible for H3K4me binding<sup>14</sup>. We therefore postulated that the human CHD1 chromodomains interact with the histone modifications associated with active chromatin; these include H3K4me, H3K36me and H3K79me as well as multiple lysine acetylations in the histone H3 tail.

We prepared a recombinant construct corresponding to the double chromodomain region (Fig. 1a) and used it for structural and biochemical studies with post-translationally modified histone H3 tails. The crystal structure in Fig. 1b, c shows the overall organization of the two chromodomains in the human CHD1 protein (Supplementary Table S1). Both chromodomains share their general secondary structure elements with those previously seen in HP1 and Polycomb chromodomains (Fig. 1d). The linker

segment forms a novel helix–turn–helix structure that juxtaposes the two chromodomains to form a continuous surface. A total of 350 Å<sup>2</sup> is buried at the interface of these tandem chromodomains.

To discover the specificity of the human CHD1 binding to methylated histone tails, we performed a series of fluorescence polarization-based assays with the use of synthetic peptides (Fig. 2a, and Supplementary Table S2). CHD1 binds only to the lysine 4-methylated H3 tail; for trimethylated lysine 4 (H3K4me3) the dissociation constant  $K_d$  is 5 μM and for monomethylated lysine 4 (H3K4me1)  $K_d$  is 17 μM. Importantly, CHD1 does not interact with the unmodified H3 tail or other histone codes associated with active chromatin, for example H3K36me or H3K79me. To understand the stereochemical basis for this specificity, we solved the crystal structure of the human CHD1 double chromodomains, in complex with the H3 tail containing both trimethyllysine and monomethyllysine at residue 4, at 2.40 and 2.65 Å resolutions, respectively (Supplementary Table S1). Difference maps showed electron density for bound H3 peptide (Fig. 2b). The trimethyllysine and monomethyllysine peptide complexes are essentially superimposable (Figs 2b and 3a).

The peptide was not located on either of the two chromodomain sites corresponding to the binding site on the HP1 and Polycomb chromodomains. Instead, the H3 tail was located at an acidic surface bridging chromodomains 1 and 2 (Fig. 2b, c). The unexpected cooperation between the CHD1 chromodomains to form a single site for peptide binding was further confirmed by isothermal titration calorimetry, which showed that their interaction involves the binding of one H3 tail to one double chromodomain polypeptide (Supplementary Fig. S1).

Peptide binding buries 475 Å<sup>2</sup> of surface on both chromodomains (Fig. 2b, c). This interaction involves residues 37, 64, 66 and 67 from chromodomain 1 and residues 150 and 166 from chromodomain 2, cooperating to bind residues 1–5 in the H3 tail (Fig. 2d), and residues 6 and 7 not forming direct contacts with either chromodomains. Figure 3a shows how the methylammonium of lysine 4 is recognized. The human CHD1 uses only two aromatic residues (tryptophans 64 and 67) for methyllysine recognition, not the three-residue aromatic cage seen previously in HP1 and Polycomb chromodomains (Fig. 3a, b)<sup>10,12</sup>. The lack of a third aromatic residue in the formation of a π-electron cage surrounding the methylammonium seems to be compensated for by an adjacent cation–π interaction involving the peptide arginine 2 and CHD1 tryptophan 67. Figure 3c shows that mutation of either tryptophan 64 or 67 to leucine substantially reduces the binding affinity for histone H3 tail methylated on lysine 4, indicating that both tryptophan residues are required for the methylammonium recognition.

However, different members of the CHD protein family exhibit

<sup>1</sup>Department of Biochemistry and Molecular Genetics, <sup>2</sup>Department of Pharmacology and <sup>3</sup>Department of Molecular Physiology and Biological Physics, University of Virginia Health System, Charlottesville, Virginia 22908, USA. <sup>4</sup>Argonne National Laboratory, Biosciences Division/Structural Biology Center, Argonne, Illinois 60439, USA. <sup>†</sup>Present address: Department of Pathology, Harvard Medical School and The CBR Institute for Biomedical Research, Inc., 200 Longwood Avenue, Boston, Massachusetts 02115, USA.

sequence variations at residue 67. In humans, three of the eight CHD proteins—CHD3 (Mi-2 $\alpha$ ), CHD4 (Mi-2 $\beta$ ) and CHD5—have a leucine or a methionine residue instead of tryptophan 67, indicating that these isoforms might not interact with the lysine 4-methylated H3 tail. Within the subfamily CHD1, the budding yeast does not have an aromatic residue at position 67 (Supplementary Fig. S2). This indicates that unlike the CHD1 from fission yeast or metazoans, the budding yeast CHD1 would not interact with the methylated H3 tail; this was confirmed in the binding studies shown in Fig. 3c and a previous report<sup>15</sup>. Thus, these data and also our studies with the isolated chromodomain 2 region of the budding yeast CHD1 (Supplementary Table S2) disagree with previous *in vitro* studies<sup>14</sup> indicating that chromodomain 2 of budding yeast CHD1 binds to the H3K4me peptide.

The intimate recognition of an arginine residue at position  $n - 2$  relative to the methyllysine carries significance for the specificity of the human CHD1 chromodomains (Fig. 3a). No other lysine methylation site in histones contains an arginine at position  $n - 2$ . Because arginine 2 can be methylated by coactivator-associated arginine methyltransferase 1 (CARM1)<sup>16</sup>, we tested whether this methylation further affected the binding of the H3 tail. Methylation

of arginine 2 (Arg 2 asymmetric dimethylation; H3R2me2a) alone does not allow binding to CHD1 chromodomains; however, this modification together with methyllysine 4 (H3K4me3R2me2a) decreased the binding affinity fourfold relative to methyllysine 4 binding alone (Fig. 3d, and Supplementary Table S2). We then solved the crystal structure of the doubly modified peptide in complex with CHD1 chromodomains (Fig. 3a) and found only one significant difference from the methyllysine 4 complex that contributes to weaker binding. Methylation of arginine 2 prevented the hydrogen bonding between its side chain and the glycine 66 backbone carbonyl (Fig. 2d).

Another modification that occurs proximal to methyllysine 4 is the phosphorylation of threonine 3. Mitotic cells preserve their lysine 4 methylation patterns to maintain active chromatin states through cell division<sup>17</sup>. Threonine 3 becomes phosphorylated during mitosis by the kinase haspin, and a lysine 4-methylated H3 tail can be phosphorylated at threonine 3 by haspin kinase *in vitro*<sup>18</sup>. These findings imply that H3K4me and H3T3ph modifications coexist during mitosis. Previous studies have indicated that CHD1 is released into the cytoplasm when cells enter mitosis<sup>19</sup>, so phosphorylation no longer supports the binding of CHD1 protein *in vivo*. Threonine 3 phosphorylation is reversed during anaphase<sup>18</sup>, and this

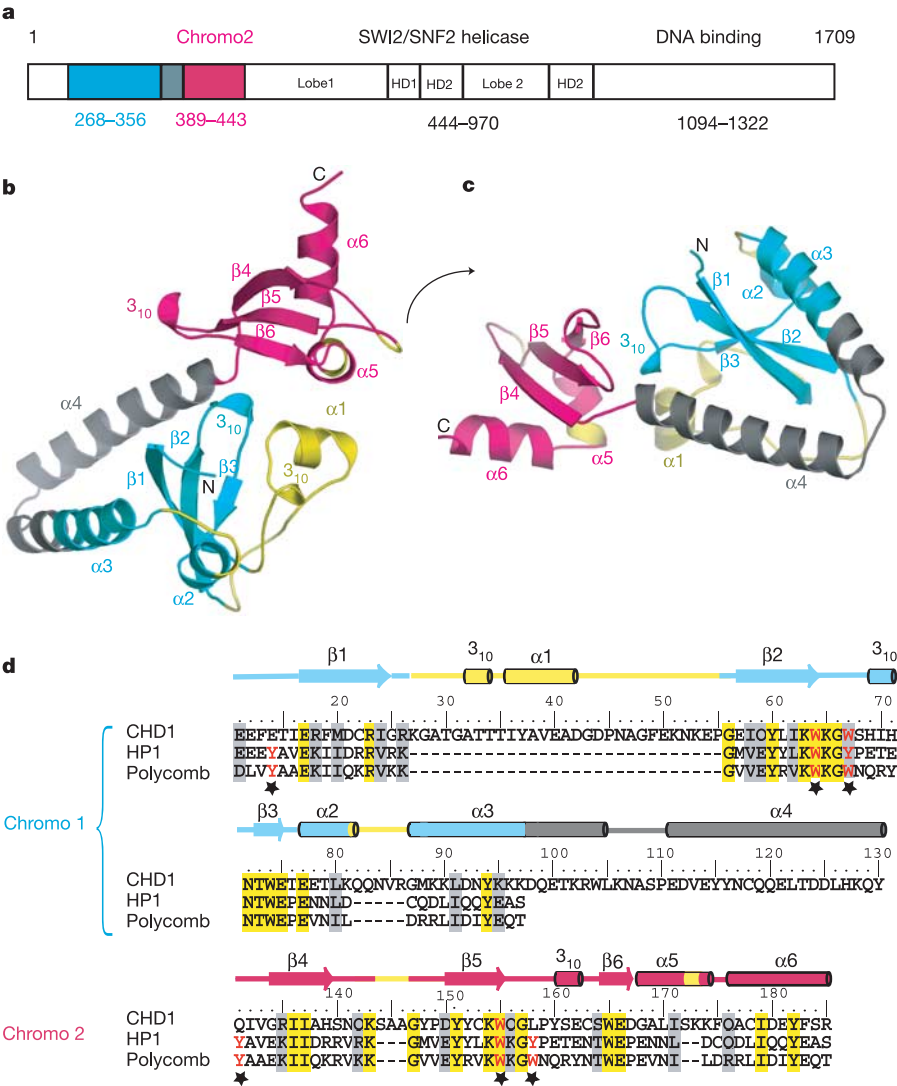


**Figure 1 | Structure of human CHD1 double chromodomains.** **a**, The conserved domains within human CHD1 sequence. The SWI2/SNF2 region is related to that of the Rad54 protein<sup>27</sup>. **b**, **c**, Crystal structure of the tandem chromodomains in two views. Cyan, chromodomain 1; grey, linker; pink, chromodomain 2; yellow corresponds to inserted sequences compared with

those of HP1 and Polycomb. **d**, Structure-based sequence alignment of CHD1 individual chromodomains with HP1 and Polycomb. The secondary structure elements above the sequence correspond to those in CHD1. The black stars indicate aromatic residues that contribute to the cage in HP1 and Polycomb.

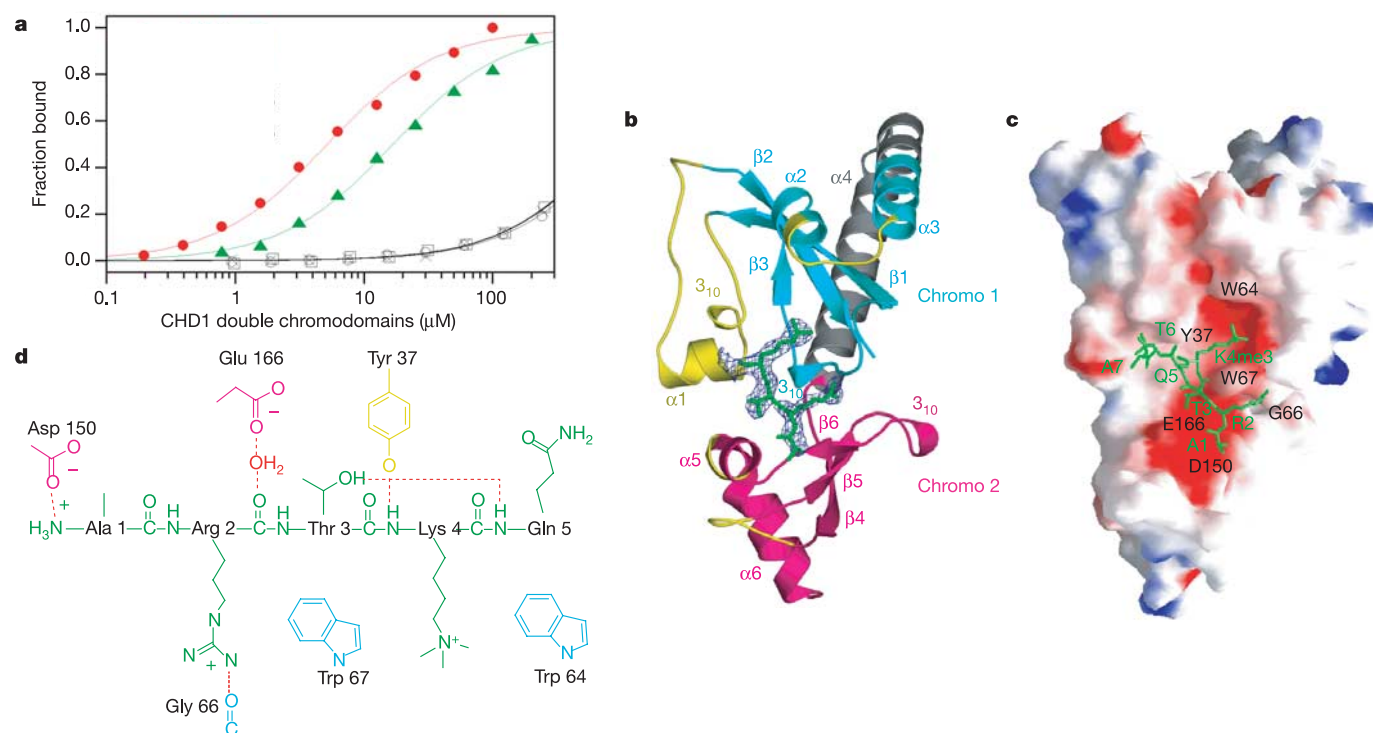


**Figure 2 | Peptide selectivity of the human CHD1 double chromodomains.** **a**, Fluorescence polarization binding assays (Supplementary Table S2). Red filled circles, H3K4me3; green triangles, H3K4me1; black crosses, H3K36me3; black squares, H3K79me3; black open circles, unmodified H3 tail. **b**, The structure of H3K4me3 bound to CHD1. Blue, electron density from an  $|F_o - F_c|$  omit map contoured at  $3\sigma$  where the H3 peptide was

omitted for the map calculation. H3 peptide is traced in green. **c**, Surface electrostatic potential showing the peptide (green)-binding groove on CHD1 (ref. 28), in the same view as in **b**. **d**, Determinants of peptide binding as seen in the structures involving H3K4me3 and H3K4me1 peptides.

dephosphorylation seems to allow CHD1 to be reincorporated into chromatin during telophase<sup>19</sup>. Lysine 4 methylation and threonine 3 phosphorylation therefore seem to act as a binary switch<sup>20</sup> for the binding of CHD1.

To further understand the effect of phosphorylation, we analysed the binding of CHD1 chromodomains to the H3 tail peptide with simultaneous phosphorylation at threonine 3 and trimethylation at lysine 4. Figure 3d shows the binding to be 25-fold weaker than the binding to methyllysine 4 alone. To understand the basis for the weaker binding we solved the structure of the complex with the doubly modified peptide (Fig. 3a). The structure shows a loss of an intrapeptide hydrogen bond between the side chain hydroxyl of threonine 3 and the backbone amide of glutamine 5 when the former is phosphorylated (Fig. 2d). The high crystallographic *B* factors in the peptide in the H3K4me3T3ph complex (Supplementary Table S1) are probably a result of the low occupancy of the peptide due to low affinity, or the reduced stability of the bound peptide conformation. More distal modifications with respect to methyllysine 4, namely acetylation or methylation of lysine 9, phosphorylation of serine 10 or acetylation of lysine 14, do not perturb the *K<sub>d</sub>* of binding to the lysine 4-methylated H3 tail (Supplementary Table S2).

The single chromodomains of HP1 and Polycomb proteins also bind to the histone H3 tail but to two other regions. HP1 binds to methyllysine 9, using residues 5–10 for specificity, whereas Polycomb binds to methyllysine 27 and using residues 20–28 for specificity. In each case the H3 tail inserts as a  $\beta$ -strand to complete the overall  $\beta$ -sandwich fold of the chromodomain in HP1 and Polycomb (Fig. 4). Figure 1d shows that CHD1 chromodomain 1 contains two significant insertions in its protein sequence relative to HP1 and Polycomb. One insertion, residues 27–55, has a clear functional role, helping to establish the peptide-binding site through tyrosine 37 (Figs 1d and 2b, d).

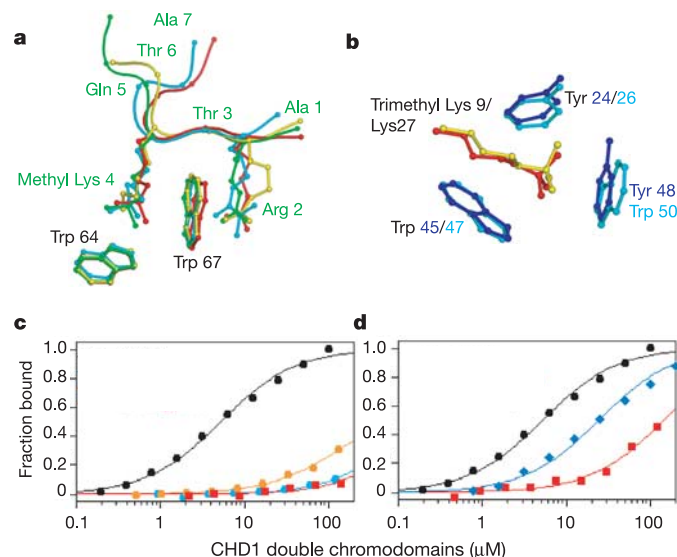


**Figure 3 | Methyllysine binding by human CHD1.** **a**, The bound-peptide structure of H3K4me3 (green), H3K4me1 (yellow), H3K4me3R2me2a (cyan) and H3K4me3T3ph (red). **b**, The aromatic cages from HP1 (blue) and Polycomb (cyan) with methyllysines 9 and 27. **c**, Fluorescence polarization peptide binding assays using human or yeast CHD1. Using H3K4me3 peptide, human CHD1 (black) binds with a *K<sub>d</sub>* of 5 μM, W67L-human CHD1 (cyan) does not bind, W64L-human CHD1 (yellow) binds with a *K<sub>d</sub>* of 290 μM, and budding yeast CHD1 (red) does not bind. W64L and W67L-human CHD1 do not allow binding to H3K4me1 or the unmodified peptide. **d**, Effect of adjacent peptide modifications. Black, H3K4me3; cyan, H3K4me3R2me2a; red, H3K4me3T3ph.



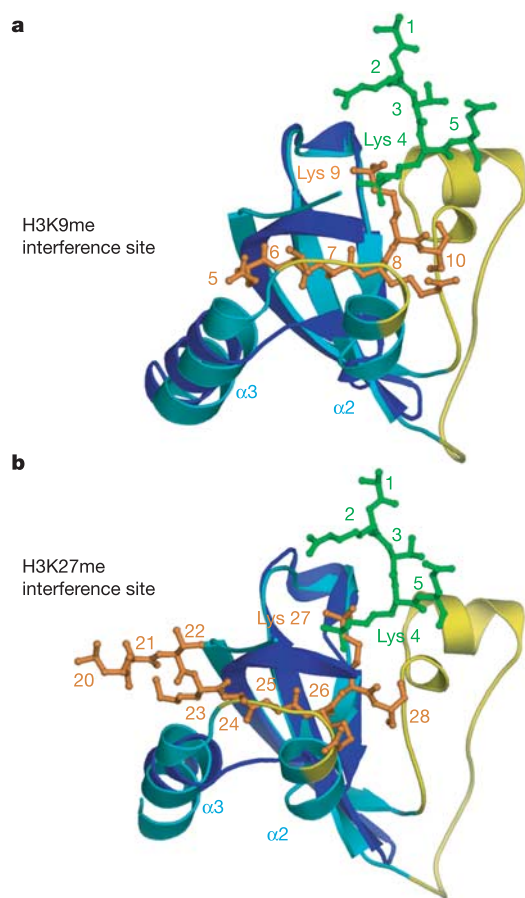


**Figure 4 | Comparison of CHD1 with HP1 and Polycomb.** **a**, HP1 chromodomain (blue) in complex with H3K9me3 (brown) superimposed on CHD1 chromodomain 1 (cyan and yellow) in complex with H3K4me3 (green). **b**, Polycomb chromodomain (blue) in complex with H3K27me3 (brown) superimposed on CHD1 chromodomain 1 (cyan and yellow) in complex with H3K4me3 (green).

There is also functional significance for the second insertion (residues 82–86) in chromodomain 1 (Fig. 1d). This insert, between helices  $\alpha 2$  and  $\alpha 3$ , occupies the site used for the recognition of the H3 tails by the HP1 and Polycomb proteins (Fig. 4). Thus, this loop blocks and interferes with the expected site of peptide interaction on chromodomain 1 of CHD1. Chromodomain 2 of CHD1 is also disabled from binding the H3 tail with the canonical interactions seen in HP1 and Polycomb, because of the availability of only one conserved aromatic residue (tryptophan 155) for binding to methyl-lysine (Fig. 1d). Because neither chromodomain alone is able to bind the peptide, the two chromodomains instead cooperate to create the recognition site.

Other conserved modules have been implicated in the recognition of post-translationally modified chromatin<sup>21</sup>, and appear in certain proteins as tandem repeats. The tandem bromodomains of TAFII250 protein bind selectively to multiply acetylated histone H4 peptides. It has been suggested that these two bromodomains form a side-by-side surface with two independent acetyllysine-binding pockets that are ideal for the recognition of one diacetylated histone H4 tail<sup>22</sup>. The 53BP1 tandem tudor domains are also implicated in binding to the core of histone H3 when lysine 79 is methylated, and it has been suggested that residues that participate in the recognition of H3 lie at the interface of the two tudor domains<sup>23</sup>. Further structure analyses involving target peptides are needed to address the significances of these double arrangements.

## METHODS

**Protein preparation.** All expression constructs contained an N-terminal His<sub>6</sub> tag, were cloned into the *Bam*HI/*Nde*I sites of the pET11a vector, expressed in BL21(DE3) *Escherichia coli* (Novagen) and purified by Ni<sup>2+</sup>-affinity chromatography (Qiagen). Point mutations were prepared with QuikChange (Stratagene). For human CHD1, the chromodomains 1 + 2 construct corresponds to residues 268–443, and the chromodomain 1 construct (with a point mutation C280S) corresponds to residues 268–362. For yeast CHD1, the chromodomains 1 + 2 construct corresponds to residues 174–339, and the chromodomain 2 construct corresponds to residues 282–339.

**Binding assays.** For fluorescence polarization, 100 nM fluorescein-labelled peptide (prepared as described previously<sup>24</sup>) was used in 50 mM sodium phosphate pH 8.0, 25 mM NaCl, 5 mM tris(2-carboxy-ethyl) phosphine (TCEP). For isothermal titration calorimetry (ITC) both protein and peptide were dialysed into 20 mM bis-tris propane (BTP) pH 8.0, 25 mM NaCl and 10 mM BME. Injections (10  $\mu$ l) of H3K4me3 peptide at 850  $\mu$ M were titrated into protein at 70  $\mu$ M concentration, with the use of a published protocol<sup>24</sup>.

**X-ray crystallography.** Crystals were prepared at 10 °C with protein samples (13.75 mg ml<sup>-1</sup>) in 20 mM BTP pH 8.0, 25 mM NaCl and 10 mM TCEP. For peptide complexes, dry peptide was added to 2.5 mM. Crystals of both free and complex grew from 6% PEG3350, 100 mM HEPES pH 8.0, and were cryo-protected in 8% PEG3350, 100 mM HEPES pH 8.0 and 35% ethylene glycol. There were 2½ molecules per asymmetric unit cell (two intact CHD1 polypeptides plus a truncation product consisting of chromodomain 1). The selenomethionyl derivative was prepared by expression in B834(DE3) *E. coli* grown in minimal media supplemented with Seleno-Met (Sigma). The structures of the free protein and complexes with peptides were determined by using the model of the H3K4me3T3ph complex solved by multiwavelength anomalous diffraction as the search model for molecular replacement (Supplementary Table S1). The program CNS was used for molecular replacement, and each model was improved by rigid body and simulated annealing refinement<sup>25</sup>. Figures were prepared with PyMOL<sup>26</sup>.

Received 12 July; accepted 4 October 2005.

- Brehm, A., Tufteland, K. R., Aasland, R. & Becker, P. B. The many colours of chromodomains. *BioEssays* **26**, 133–140 (2004).
- Tajul-Arifin, K., Teasdale, R., Ravasi, T., Hume, D. A. & Mattick, J. S. Identification and analysis of chromodomain-containing proteins encoded in the mouse transcriptome. *Genome Res.* **13**, 1416–1429 (2003).
- Lusser, A., Urwin, D. L. & Kadonaga, J. T. Distinct activities of CHD1 and ACF in ATP-dependent chromatin assembly. *Nature Struct. Mol. Biol.* **12**, 160–166 (2005).
- Bouazoune, K. *et al.* The dMi-2 chromodomains are DNA binding modules important for ATP-dependent nucleosome mobilization. *EMBO J.* **21**, 2430–2440 (2002).
- Woodage, T., Basrai, M. A., Baxevanis, A. D., Hieter, P. & Collins, F. S. Characterization of the CHD family of proteins. *Proc. Natl Acad. Sci. USA* **94**, 11472–11477 (1997).
- Stokes, D. G., Tartof, K. D. & Perry, R. P. CHD1 is concentrated in interbands and puffed regions of *Drosophila* polytene chromosomes. *Proc. Natl Acad. Sci. USA* **93**, 7137–7142 (1996).
- Tong, J. K., Hassig, C. A., Schnitzler, G. R., Kingston, R. E. & Schreiber, S. L. Chromatin deacetylation by an ATP-dependent nucleosome remodelling complex. *Nature* **395**, 917–921 (1998).
- Zhang, Y., LeRoy, G., Seelig, H. P., Lane, W. S. & Reinberg, D. The dermatomyositis-specific autoantigen Mi2 is a component of a complex containing histone deacetylase and nucleosome remodeling activities. *Cell* **95**, 279–289 (1998).
- Schneider, R. *et al.* Histone H3 lysine 4 methylation patterns in higher eukaryotic genes. *Nature Cell Biol.* **6**, 73–77 (2004).
- Jacobs, S. A. & Khorasanizadeh, S. Structure of the HP1 chromodomain bound to a lysine 9-methylated histone H3 tail. *Science* **295**, 2080–2083 (2002).
- Nielsen, P. R. *et al.* Structure of the HP1 chromodomain bound to histone H3 methylated at lysine 9. *Nature* **416**, 103–107 (2002).
- Fischle, W. *et al.* Molecular basis for the discrimination of repressive methyl-lysine marks in histone H3 by Polycomb and HP1 chromodomains. *Genes Dev.* **17**, 1870–1881 (2003).
- Min, J., Zhang, Y. & Xu, R. M. Structural basis for specific binding of Polycomb chromodomain to histone H3 methylated at Lys 27. *Genes Dev.* **17**, 1823–1828 (2003).
- Pray-Grant, M. G., Daniel, J. A., Schieltz, D., Yates, J. R. & Grant, P. A. Chd1 chromodomain links histone H3 methylation with SAGA- and SLIK-dependent acetylation. *Nature* **433**, 434–438 (2005).
- Santos-Rosa, H. *et al.* Methylation of histone H3 K4 mediates association of the Isw1p ATPase with chromatin. *Mol. Cell* **12**, 1325–1332 (2003).
- Schurter, B. T. *et al.* Methylation of histone H3 by coactivator-associated arginine methyltransferase 1. *Biochemistry* **40**, 5747–5756 (2001).

17. Kouskouti, A. & Talianidis, I. Histone modifications defining active genes persist after transcriptional and mitotic inactivation. *EMBO J.* **24**, 347–357 (2005).
18. Dai, J., Sultan, S., Taylor, S. S. & Higgins, J. M. The kinase haspin is required for mitotic histone H3 Thr 3 phosphorylation and normal metaphase chromosome alignment. *Genes Dev.* **19**, 472–488 (2005).
19. Stokes, D. G. & Perry, R. P. DNA-binding and chromatin localization properties of CHD1. *Mol. Cell. Biol.* **15**, 2745–2753 (1995).
20. Fischle, W., Wang, Y. & Allis, C. D. Binary switches and modification cassettes in histone biology and beyond. *Nature* **425**, 475–479 (2003).
21. Khorasanizadeh, S. The nucleosome: from genomic organization to genomic regulation. *Cell* **116**, 259–272 (2004).
22. Jacobson, R. H., Ladurner, A. G., King, D. S. & Tjian, R. Structure and function of a human TAF<sub>II</sub>250 double bromodomain module. *Science* **288**, 1422–1425 (2000).
23. Huyen, Y. *et al.* Methylated lysine 79 of histone H3 targets 53BP1 to DNA double-strand breaks. *Nature* **432**, 406–411 (2004).
24. Jacobs, S. A., Fischle, W. & Khorasanizadeh, S. Assays for the determination of structure and dynamics of the interaction of the chromodomain with histone peptides. *Methods Enzymol.* **376**, 131–148 (2004).
25. Brunger, A. T. *et al.* Crystallography and NMR system: A new software suite for macromolecular structure determination. *Acta Crystallogr. D* **54**, 905–921 (1998).
26. DeLano, W. L. *PyMOL User's Guide* (DeLano Scientific, San Carlos, California, 2004).
27. Thoma, N. H. *et al.* Structure of the SWI2/SNF2 chromatin-remodeling domain of eukaryotic Rad54. *Nature Struct. Mol. Biol.* **12**, 350–356 (2005).
28. Nicholls, A. *GRASP: Graphical Representation and Analysis of Surface Properties* (Columbia University, New York, 1993).

**Supplementary Information** is linked to the online version of the paper at [www.nature.com/nature](http://www.nature.com/nature).

**Acknowledgements** We thank M. Zimmerman for assistance with diffraction data collection. This work was supported by grants from the National Institutes of Health (to S.K.).

**Author Contributions** J.F.F. and L-Z.M. contributed equally to this work.

**Author Information** The atomic coordinates have been deposited in the Protein Data Bank with the accession numbers 2B2Y, 2B2W, 2B2V, 2B2U and 2B2T. Reprints and permissions information is available at [npg.nature.com/reprintsandpermissions](http://npg.nature.com/reprintsandpermissions). The authors declare no competing financial interests. Correspondence and requests for materials should be addressed to S.K. ([khorasan@virginia.edu](mailto:khorasan@virginia.edu)) or F.R. ([fr9c@virginia.edu](mailto:fr9c@virginia.edu)).